

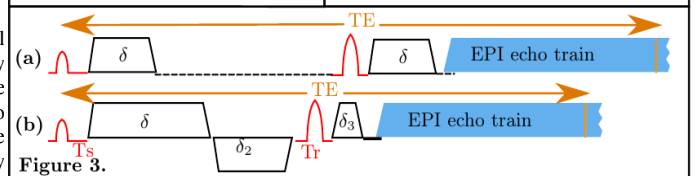
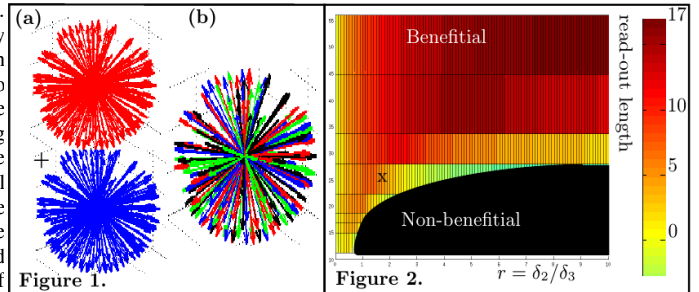
# Optimized multi-shell HARDI acquisition with alternating phase encoding directions for neonatal dMRI

Jana Hutter<sup>1,2</sup>, Jacques-Donald Tournier<sup>1</sup>, Emer J. Hughes<sup>1</sup>, Anthony N. Price<sup>1</sup>, Lucilio Cordero-Grande<sup>1,2</sup>, Rita G. Nunes<sup>1</sup>, Rui Pedro A. G. Teixeira<sup>1,2</sup>, Serena J. Counsell<sup>1</sup>, Jesper L. R. Andersson<sup>3</sup>, Daniel Rueckert<sup>4</sup>, A. David Edwards<sup>1,2</sup>, and Jo V. Hajnal<sup>1,2</sup>

<sup>1</sup>Centre for the Developing Brain, King's College London, London, London, United Kingdom, <sup>2</sup>Division of Imaging Sciences and Biomedical Engineering, King's College London, London, London, United Kingdom, <sup>3</sup>FMRI, Oxford, Oxfordshire, United Kingdom, <sup>4</sup>Biomedical Image Analysis Group, Department of Computing, Imperial College London, London, United Kingdom

**Introduction:** The demands of diffusion MRI (dMRI) acquisition continue to increase as biophysical modeling (1), connectomics (2) and other advanced analyses emerge. Recently the Human Connectome Project (3,4) addressed these challenges by developing a protocol comprising 3 b-value shells, each with about 90 sensitization directions ( $b_{\text{vecs}}$ ) and every image acquired twice with reversed phase encoding (PE) to ensure all regions are fully encoded (balancing spatial collapse vs stretching). The whole protocol takes 60 minutes and the volunteers are trained. For the developing Human Connectome Project (dHCP) we aspire to acquire data of as closely comparable data quality as possible to study brain development in 1000 neonates imaged in natural sleep. The total acquisition time is limited to about 20 minutes and neonates are prone to sporadic movements that may damage individual acquired images. In this work we explored strategies to optimize dMRI by reducing the echo time to increase SNR and creating an integrated interleaved acquisition scheme that combines diversity of encoding with robustness to sporadic data loss.

**Methods:** For a given b-value with given gradient system performance, the temporal efficiency of single-shot pulse gradient echo-planar imaging (PG-EPI) is critically dependent on the duration of the EPI readout required to achieve the desired image resolution (Figure 3a). Keeping the same readout and diffusion weighting, the echo time (TE) can be reduced by moving part of the second gradient lobe before the refocusing RF pulse as shown in figure 3b. This has the advantage of decreasing eddy currents (5,6) but can result in signal loss due to concomitant gradients (7); fortunately the latter effect is negligible for neonatal brains as distance from the scanner isocentre is invariably smaller than 10 cm. Figure 2 shows the reduction in TE for 80mT/m gradients when  $b=2500\text{s/mm}^2$ . The related optimization problem, minimizing the echo time, while achieving a set b-value  $b$ , respecting hardware and crushing constraints, given in Eq. 1, and was implemented within the sequence calculation to achieve minimal TE. To enhance acquisition efficiency and robustness to data loss from sporadic motion, separate complete acquisitions with reversed PE (Figure 3a) are replaced by a fully interleaved acquisition in which the b value, direction of sensitization ( $b_{\text{vec}}$ ) and phase encode direction can be freely selected for each acquired stack of EPI images (Figure 3b in which PE direction is color coded). A triple interleaved optimization scheme is used to design the sequence: A spherically optimized set of directions, in fixed scanner geometry to enhance the comparability between subjects, is generated using electrostatic repulsion and then split into 4 subsets (one per PE direction) with maximal intra-subset electrostatic repulsion, as shown in Fig. 1b in which each color denotes a different PE direction. Finally, these directions are spread temporally such that the time between close sensitization directions with the same phase encoding is maximized. To minimize total acquisition time, the sequence is made fully self-sufficient by including all required calibration information, duty cycle considerations that take account of the highly variable demand on each gradient axis and PNS checks. The optimized sequence has been implemented on a clinical 3T Philips Achieva system operating at 80mT/m on each axis and tested using phantoms, adults scanned in a 32 channel head coil and neonates examined using a dedicated 32-channel neonatal head coil (RAPID Biomedical, Germany) for optimal SNR.

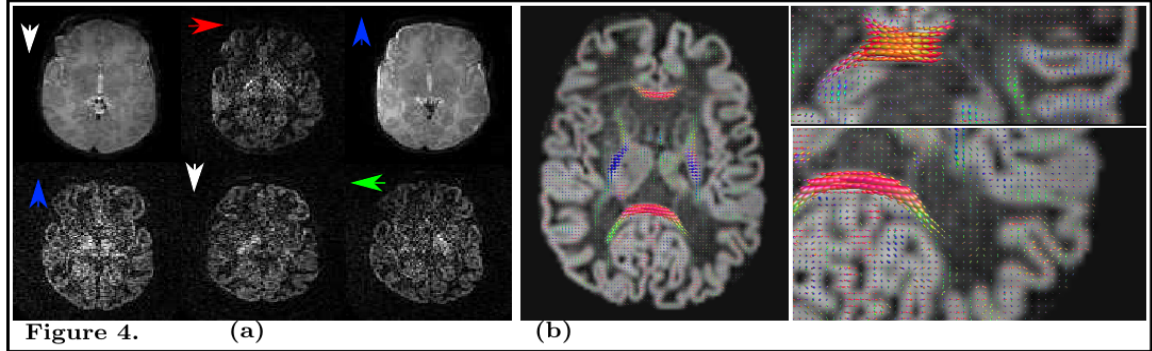


**Eq. 1**  $(\hat{r}, \hat{\delta}_2) = \underset{r, \delta_2}{\operatorname{argmin}} TE(G, \gamma, T_s, Tr, s, r, \delta_2)$  such that

$$\gamma^2 G^2 [\delta_1^2 (\Delta - \frac{\delta_1}{3}) + \delta_3^2 Tr - \frac{1}{6} \delta_1^2 s^2 + \frac{1}{20} s^3] = b$$

where  $\Delta = \frac{TE}{2} - \frac{Tr}{2} - Ts - \delta_2$ ,  $\delta_3 = \frac{\delta_2}{r}$  and  $\delta_1 = \delta_2 + \delta_3$

As shown in Fig. 1b in which each color denotes a different PE direction. Finally, these directions are spread temporally such that the time between close sensitization directions with the same phase encoding is maximized. To minimize total acquisition time, the sequence is made fully self-sufficient by including all required calibration information, duty cycle considerations that take account of the highly variable demand on each gradient axis and PNS checks. The optimized sequence has been implemented on a clinical 3T Philips Achieva system operating at 80mT/m on each axis and tested using phantoms, adults scanned in a 32 channel head coil and neonates examined using a dedicated 32-channel neonatal head coil (RAPID Biomedical, Germany) for optimal SNR.



The optimized sequence has been implemented on a clinical 3T Philips Achieva system operating at 80mT/m on each axis and tested using phantoms, adults scanned in a 32 channel head coil and neonates examined using a dedicated 32-channel neonatal head coil (RAPID Biomedical, Germany) for optimal SNR.

**Results and Discussion:** Figure 2 presents the achievable new ranges of echo times for a b-value of 2500 s/mm<sup>2</sup> using the split gradient scheme, a maximum gradient strength of 80 mT/m and a matrix size of 128 x 128 for the fully sampled case for different choices of SENSE and partial Fourier factor and the ratio r (see Fig 2). It shows that a beneficial setting with the new choice is achievable for every read-out length with a peak of 17ms echo time reduction for full k-space sampling. The proposed optimized neonatal dMRI sequence was successfully validated in phantom scans and adults, confirming stability and that the required b-value/directions were obtained. The entire sequence was then successfully applied to 5 preterm and term neonatal subjects (gestational age 34+5, 37+3, 40, 40+1 and 43+3 weeks). The parents gave written consent prior to scanning. Results from a high-resolution neonatal acquisition using a FOV of 160 x 160, SENSE 2, partial Fourier of 0.9, TR=7428ms, isotropic resolution 1.25 mm<sup>3</sup> with 44 non-collinear directions with  $b=2500\text{s/mm}^2$  and 4 interleaved b0s are shown in Fig. 4. The echo time was reduced from 88ms to 79ms compared to the standard PGSE case. All images were distortion-corrected using the FSL's EDDY command (8,9) and processed using constrained spherical deconvolution in MRtrix (10). The unprocessed images are shown in 4a to illustrate the high information content achieved in a single 6 minute scan: in 4b, the fiber orientation density result obtained after combining all directions, after processing: note the clear depiction of the expected radial fibre arrangement in the cortex, and the high apparent fibre density in the major white matter tracts (corpus callosum, corticospinal tract, optic radiations). The presented sequence optimizations offer an integrated single scan solution producing highly eloquent, minimal TE data. The resulted flexibility in timing is especially beneficial when combined with multi-band acceleration (11) techniques, which will be part of the dHCP acquisitions.

**Acknowledgments:** The authors acknowledge funding from the MRC strategic funds, GSTT BRC and the ERC funded dHCP project.

**References:** [1] Zhang, Neuroimage:61(4):1000-16 (2012) [2] Hagmann, Jour of Neuro Meth:194:34-45 (2010) [3] Sotiropoulos, Neuroimage 80:125-143 (2013) [4] Ugurbil, NeuroImage 80:80-104 (2013) [5] Finsterbusch, MRM 61:748-754 (2009) [6] Nunes, Magnetic Resonance Imaging 29:5 : 659-667 (2011) [7] Baron, Magn Reson Med:68:4:1190-201 (2012) [8] Smith et al., NeuroImage:23:1:208-219 (2004), [9] Andersson, NeuroImage:20:2:870-888 (2013), [10] Tournier, Int. J. of I. Sys. and Technology 22:1:53-66 (2012), [11] Moeller, MRM:63:1144-53 (2009)